Activated Nucleation of Vortices in a Dipole-Blockaded Supersolid Condensate

Peter Mason,[1] Christophe Josserand,[2] and Sergio Rica[3]

[1]Department of Physics, Durham University, Durham DH1 3LE, United Kingdom
[2]Institut Jean Le Rond D'Alembert, UMR 7190 CNRS-UPMC, 4 Place Jussieu, 75005 Paris, France
[3]Facultad de Ingeniería y Ciencias, Universidad Adolfo Ibáñez, Avda. Diagonal las Torres 2640, Peñalolén, Santiago, Chile

(Received 28 February 2012; published 23 July 2012)

We investigate theoretically and numerically a model of a supersolid in a dipole-blockaded Bose-Einstein condensate. The dependence of the superfluid fraction with an imposed thermal bath and a uniform boost velocity on the condensate is considered. Specifically, we observe a critical velocity for the nucleation of vortices in our system that is strongly linked to a steplike decrease in the superfluid fraction. We are able to use a scaling argument based on the energy required to activate a vortex, relating the critical temperature to the critical velocity, and find that this relationship is in good agreement with the numerical simulations carried out on the nonlocal Gross-Pitaevskii equation.

DOI: 10.1103/PhysRevLett.109.045301 PACS numbers: 67.80.K−, 67.30.he, 67.80.bd

A Bose-Einstein condensate (BEC) is one of the fundamentally important theoretical and experimental discoveries in the field of ultracold atoms. It is the condensation, or transition, of boson atoms into the lowest available quantum state, representing a new state of (coherent) matter. As part of their seminal paper linking Bose-Einstein condensation to off-diagonal long-range order, Penrose and Onsager [1] were one of the first to consider theoretically the possibility of a superfluidlike behavior in a solid ^{4}He crystal—the appearance of a supersolid. They noticed, crucially, that the number of particles per site can fluctuate implying an off-diagonal long-range order.

The existence or not of the supersolid, a state of matter in which the solid has crystalline order and in which there is dissipationless flow, is not clear. Early experiments trying to measure a superflow generated in solid helium were unsuccessful [2], and it was not until recently that Kim and Chan [3–5] presented the first experimental evidence for the existence of a supersolid. These authors measured the effective rotational inertia of the solid helium sample, noting that there was an observable drop in its value that would be a result of the decoupling of a superfluid component (that remains motionless) from the solid crystal. This, termed the nonclassical rotational inertia (NCRI), is the strongest evidence yet for the existence of a supersolid. While these experiments have been much reproduced [6–9], another line of experiment has been to focus on particular aspects of the helium sample, such as the annealing process or the measurement of the shear modulus, which might suggest another explanation for the apparent existence of the supersolid phase. The annealing process has been shown to dramatically reduce the superfluid fraction [10,11], while the shear modulus displays a similar dependence to the NCRI [12].

Related to this, recent experimental results on supersolid helium have suggested a strong interplay between rotation and relaxation [13]. There, the supersolid fraction decreases with increasing temperature and rotation frequency in a specific way, even if in this case the role of the torsion rod is questioned [12,14]. The existence of a supersolid, thus, remains an open and vibrant question.

Instead of looking to supersolidity in solid helium, one might gain some insight through similar processes in cold atoms as provided by the recently achieved BEC in dipole-blockaded Rydberg atoms [15]. The aim of our Letter is precisely to investigate the effects of an imposed rotation and temperature field on the superfluid fraction in a model of a supersolid that has been developed for the dipole-blockaded BEC [16]. In the configuration proposed here, the atoms are confined and form a two-dimensional (2D) gas. Despite this confinement, the mean-field energy of dipolar interactions conserves a $1/r^3$ long-range behavior (see Supplemental Material [17]). Moreover, the Bogoliubov excitation spectrum exhibits a roton minimum near the inverse of the thickness of the confinement [18]. The effective 2D two-body potential is, thus, composed of a long-distance repulsion together with a short-distance cutoff. Qualitatively, the results do not depend strongly on the explicit form of this potential, and we shall consider a simpler form: $U(r) = V_0$ if $r \leq a$ and $U(r) = V_0 \frac{a^3}{r^3}$ if $r > a$. Here, $r^2 = x^2 + y^2$, V_0 is the characteristic strength of interactions and a the characteristic length scale of the potential allowing for the appearance of a roton spectrum [16,19,20]. The existence of this roton minimum depends on the number density and the model parameters V_0 and a (see the dimensionless parameter Λ (4) defined below). From an experimental point of view, the control parameter is V_0 which can be easily increased since it depends strongly on the quantum number of the Rydberg state. Then, the system spontaneously breaks the translational invariance leading to the appearance of a crystalline phase of individual superfluid droplets governed by a global macroscopic wave function. This system, by supporting a density modulation, can naturally exhibit supersolid behavior, notably the decoupling of a superfluid component from

the crystalline structures. As such, the Rydberg excited atoms can give rise to supersolid behavior directly in a BEC and can then potentially provide useful insights into the nature of the supersolid phase in solid helium. In this framework, we will show that thermal activation of superfluid vortices is the physical mechanism governing the superfluid dependence on the temperature and the imposed velocity, in contrast with the self-similar structure found in [13].

Because of its condensate structure, and contrary to the case of ^{4}He, the dynamics of dipole-blockaded Rydberg atoms can be investigated within the mean-field approximation leading to a nonlocal Gross-Pitaevskii (GP) equation that describes the 2D (x, y) Bose gas in terms of the classical complex wave function $\psi(\boldsymbol{x}, t)$ in the zero temperature limit,

$$i\hbar\frac{\partial\psi}{\partial t} = -\frac{\hbar^2}{2m}\nabla^2\psi + \psi\int U(|\boldsymbol{x}-\boldsymbol{x}'|)|\psi(\boldsymbol{x}', t)|^2 d\boldsymbol{x}'. \quad (1)$$

Here $\hbar$ is Planck's constant, m is the mass of the boson, $U(r)$ is the aforementioned two-body potential, and the integration is over the whole plane. The GP equation has a Hamiltonian structure ($i\hbar\partial_t\psi = \delta H/\delta\psi^*$ with $H[\psi] = \int\frac{\hbar^2}{2m}|\nabla\psi|^2 d\boldsymbol{x} + \frac{1}{2}\int U(|\boldsymbol{x}-\boldsymbol{x}'|)|\psi(\boldsymbol{x}, t)|^2|\psi(\boldsymbol{x}', t)|^2 d\boldsymbol{x}d\boldsymbol{x}'$) so that together with the energy, the total number of bosons, N, and the momentum, $\boldsymbol{P}$, given as

$$N = \int|\psi|^2 d\boldsymbol{x}, \quad \boldsymbol{P} = -\frac{i\hbar}{2}\int(\psi^*\boldsymbol{\nabla}\psi - \psi\boldsymbol{\nabla}\psi^*)d\boldsymbol{x}, \quad (2)$$

are conserved. The values of V_0 and a determine whether the Bose gas has a modulated density or not. To see this more clearly, it is better to move to nondimensional fields. Thus, we set $\boldsymbol{x} = a\tilde{\boldsymbol{x}}$, $t = ma^2\tilde{t}/\hbar$ and $\psi = \sqrt{n_0}\tilde{\psi}$, where n_0 is a mean density. The nondimensional GP equation is then (dropping tildes hereafter)

$$i\frac{\partial\psi}{\partial t} = -\frac{1}{2}\nabla^2\psi + \Lambda\psi\int V(|\boldsymbol{x}-\boldsymbol{x}'|)|\psi(\boldsymbol{x}', t)|^2 d\boldsymbol{x}'. \quad (3)$$

The system has been reduced to a single free nondimensional parameter [21]

$$\Lambda = 3\pi\frac{n_0 m a^4 V_0}{\hbar^2} \quad (4)$$

with

$$V(r) = \frac{1}{3\pi}\begin{cases} 1 & \text{if } r \le 1 \\ 1/r^3 & \text{if } r > 1 \end{cases}. \quad (5)$$

Linear perturbations around the homogeneous solution $\psi_0 = e^{-i\Lambda t}$ give the dispersion relationship between the frequency ω_k and the wave number k as [22]

$$\omega_k = \sqrt{k^4/4 + \Lambda k^2\hat{V}_k}, \quad (6)$$

where $\hat{V}_k = \int_0^\infty\int_0^{2\pi} V(r)e^{ikr\cos\theta}rdrd\theta$ (bounded for all k) is the Fourier transform of $V(r)$.

For the Bose-Einstein condensate with two-body potential determined through the Born approximation, the frequency is a monotonically increasing function of k ($\hat{V}_k = 1$) and does not contain a roton component. This prevents the condensate forming a density modulation. In contrast, in the case of dipole-blockaded Rydberg atoms and more generally when long-range interactions are present, the Fourier transform V_k has negative values for a range of wave numbers which allows a roton spectrum to develop. The appearance of this roton spectrum is controlled by the value of the free parameter Λ, which enhances the negative part of V_k, as shown in Fig. 1. Once the roton spectrum becomes of significant strength, we can expect a density modulation of the ground state to form.

This ground state of the system is determined numerically by minimizing the energy functional subject to the constraint on the number of particles in the system. In general, this solution exists and is real (although later considerations involving the addition of an imposed velocity and temperature will produce a complex solution). When Λ is small, the ground state is homogeneous in space (i.e., it has no positional order). As Λ increases, the ground state exhibits a first-order phase transition for a critical value Λ_c, above which a density modulated solution is preferred that is brought about through the competition between the nonlocal interaction and the kinetic energy. For the system presented above, $\Lambda_c \sim 89.85$ and the insert of Fig. 1 illustrates such a density modulated ground state, a hexagonal crystal, for $\Lambda = 152.68$. Using the experimental values for Rydberg states of ^{87}Rb described in [15], such Λ could be achieved for a 2.5 μm thick condensate, with $a = 400$ nm, $V_0 = 17$ nK, and a dimensionless density $n_0a^2 \approx 32$. Similarly, the numerical simulations of [16] (see their Fig. 1) were realized with, using their notation, $\Lambda = 3\pi R_c/r_s^2 = 144$, which is also a crystalline state regime.

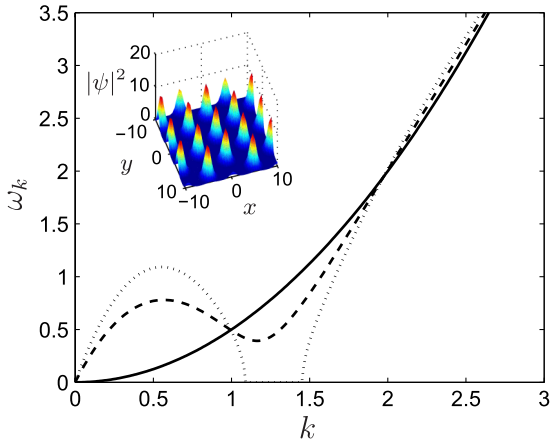

FIG. 1 (color online). A plot of the real part of the dispersion relationship (6) for varying values of Λ (solid line: $\Lambda = 0$, dashed line: $\Lambda = 76.34$, and dotted line: $\Lambda = 152.68$). Inset: A density modulated ground state with $\Lambda = 152.68$.

Because of its condensate feature, such a crystal naturally exhibits supersolidity; i.e., it possesses a nonzero NCRI. As has previously been shown [23–25] for a similar model of a supersolid as we take here (but with a soft core potential), a crystal in rotation will give a nonzero NCRI. Equivalently, but with better numerical accuracy, one can consider instead the momentum of the crystal under a Galilean boost $\boldsymbol{v}$ [25,26], yielding

$$i\frac{\partial\psi}{\partial t} = -\frac{1}{2}\nabla^2\psi + \Lambda\psi\int V(|\boldsymbol{x}-\boldsymbol{x}'|)|\psi(\boldsymbol{x}',t)|^2 d\boldsymbol{x}' + i\boldsymbol{v}\cdot\boldsymbol{\nabla}\psi. \tag{7}$$

Thus, by measuring the linear momentum of the solution, one can define equivalently the supersolid density fraction tensor f_{ss} as

$$f_{ss}\boldsymbol{v} = \boldsymbol{v} - \frac{\boldsymbol{P}}{N}. \tag{8}$$

This tensor can be assumed to be symmetric and the diagonal value of the tensor, which is precisely the supersolid fraction, has been shown to decrease monotonically with Λ [23,25,27].

Although the GP formulation assumes that the Bose gas is held at zero temperature, thermal effects can be accounted for in the frame of the time-dependent Ginzburg-Landau model [28] by adding a complex white noise $\eta(\boldsymbol{x},\tau)$ to the dynamics following [29–31]. Thus,

$$\frac{\partial\psi}{\partial\tau} = \mu\psi + \frac{1}{2}\nabla^2\psi - \Lambda\psi\int V|\psi(\boldsymbol{x}',\tau)|^2 d\boldsymbol{x}' - iv\frac{\partial\psi}{\partial x} - \sqrt{2T}\eta, \tag{9}$$

with $\langle\eta(\boldsymbol{x},\tau)\rangle = 0$ and $\langle \mathrm{Re}[\eta(\boldsymbol{x},\tau)]\mathrm{Re}[\eta(\boldsymbol{x}',\tau')]\rangle = \langle \mathrm{Im}[\eta(\boldsymbol{x},\tau)]\mathrm{Im}[\eta(\boldsymbol{x}',\tau')]\rangle = \delta(\boldsymbol{x}-\boldsymbol{x}')\delta(\tau-\tau')$, with T the temperature and considering, for the sake of simplicity, a boost v solely in the x direction because of symmetry. Thus, we resort to a numerical simulation on the GP equation in imaginary time, $t = -i\tau$, introducing a chemical potential μ to satisfy the mass conservation. With the present normalization, the amplitude of the fluctuations T has the same units as the Hamiltonian and this stochastic process has a Gibbs equilibrium probability distribution $p \sim e^{-(H-\boldsymbol{v}\cdot\boldsymbol{P})/T}$.

4In order to study the supersolid fraction as a function of both the velocity and the temperature (for a fixed value of $\Lambda = 106.88$), we look for stationary solutions of Eq. (9). Our numerical simulations are carried out on a discretized 256×256 grid with $dx = 0.5$ to reach good numerical accuracy and with periodic boundary conditions on the four sides. The starting numerical solution from which we iterate is the zero velocity and temperature solution (see Fig. 1). For each iteration of the velocity and the temperature, we compute the supersolid fraction using Eq. (8) after a stationary regime has been reached. In Fig. 2 we show a 3D plot of the superfluid fraction as a function of the velocity and temperature. We see that the superfluid fraction is affected by both the velocity and the temperature through sudden variations, as can be seen clearly in Figs. 3(a) and 3(b). These figures show a slice of the superfluid fraction against velocity while the temperature is fixed [Fig. 3(a)] or against temperature while the velocity is fixed [Fig. 3(b)]. The superfluid fraction exhibits steplike decreases that correspond to the occurrence of a phase slip in the wave function that lowers the superfluid fraction since it induces a global boost to the solution.

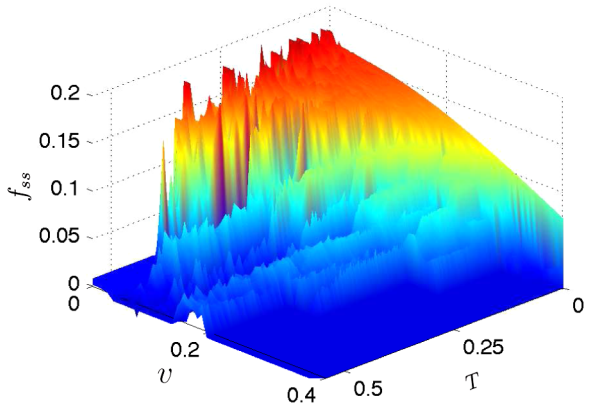

FIG. 2 (color online). A plot of the superfluid fraction f_{ss} (vertical axis) against velocity and temperature.

Such a phase slip can be observed in Fig. 4(a), where a horizontal cut of the phase is shown for two different temperatures $T = 1.08\times10^{-4}$ and $T = 0.012$ for the same velocity $v = 0.25$ as indicated by the two crosses of Fig. 3(b). For $T = 1.08\times10^{-4}$, the phase exhibits a periodic pattern while for $T = 0.012$ a 2π phase slip is present as shown by the phase jump, due to the 2π-periodic definition of the phase. This phase jump appears for an almost constant x isoline in the phase plot of the solution shown in Fig. 4(b). Notice that a 2π phase jump would correspond to a quantized vortex of charge one in the

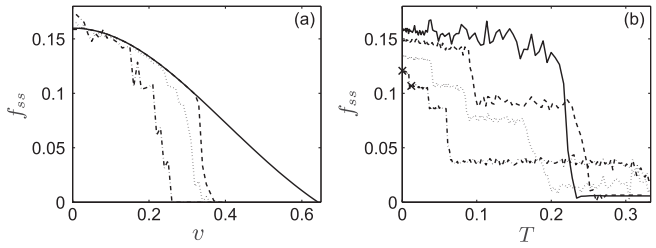

FIG. 3. A plot of the superfluid fraction f_{ss} against (a) velocity when the temperature field is varied: $T = 0$ (solid line), $T = 1.08\times10^{-4}$ (dashed line), $T = 0.015$ (dotted line), and $T = 0.06$ (dashed-dotted line) and (b) temperature when the velocity field is varied: $v = 0.05$ (solid line), $v = 0.13$ (dashed line), $v = 0.2$ (dotted line), and $v = 0.25$ (dashed-dotted line). The crosses correspond to $v = 0.25$ and $T = 1.08\times10^{-4}$ and $T = 0.012$ showing activation of a phase slip, as in Fig. 4.

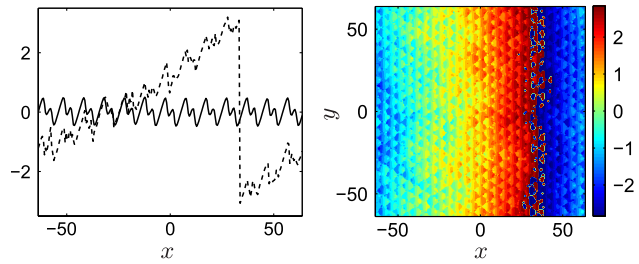

FIG. 4 (color online). The phase profile (left plot) of the wave function for $T = 1.08 \times 10^{-4}$ (solid line) and $T = 0.012$ (dashed line) and a contour plot (right plot) for $T = 0.012$. A phase slip appears around $x = 33.5$. In all cases $v = 0.25$.

annular geometry under rotation. Moreover, as T increases, other jumps can be identified in Fig. 3(b) due to the successive nucleation of vortices.

This rapid decrease of the superfluid fraction as T and v increase thus allows for a natural definition of a critical velocity (function of the temperature) of the supersolid, and we will now demonstrate that the vortices are nucleated through a thermally activated process according to the aforementioned Gibbs probability factor. Indeed, following the classical argument given by Fisher and Langer [32], we consider the energy of a pair of counterrotating vortices separated by a distance R in a moving superfluid of density ϱ^{ss} [33] at speed v (for physical relevance, the discussion below comes back to physical units),

$$\mathcal{E}(R) = E_v - \boldsymbol{v}\cdot\boldsymbol{P} = \pi\frac{\hbar^2}{m}\varrho^{ss}\log(R/a_0) - \pi\hbar v\varrho^{ss}R,$$

where the length a_0 corresponds to the size of the vortex core and in superfluids is related to the healing length $a_0 \sim 1/\sqrt{\varrho^{ss}}$. This energy is maximal for a critical distance $R_* = \frac{\hbar}{mv}$ which corresponds clearly to an unstable configuration: while the two vortices would collapse if $R < R_*$, they will separate for $R > R_*$, thus leading to the occurrence of vortices within the flow. The energy barrier for vortex nucleation follows from

$$\Delta\mathcal{E} = \mathcal{E}(R_*) - \mathcal{E}(a_0) = \pi\frac{\hbar^2}{m}\varrho^{ss}\left[\log\left(\frac{v_0}{v}\right) - 1 + \left(\frac{v}{v_0}\right)\right], \tag{10}$$

introducing the typical velocity $v_0 = \frac{\hbar}{ma_0}$. In a thermal activated process, the probability for vortex nucleation is proportional to the Arrhenius factor $e^{-\Delta\mathcal{E}/T}$, which gives the link between the critical velocity v_c and the temperature

$$\varrho^{ss}\left[\log\left(\frac{v_0}{v_c}\right) - 1 + \left(\frac{v_c}{v_0}\right)\right] \propto T_c. \tag{11}$$

This relation is in good agreement with the numerical results obtained above as shown in Fig. 5, where the velocity contour plot, for $\varrho^{ss} \approx 0.1$, is compared with the above formula with $v_0 = 0.35$ and the constant of proportionality $\kappa = 0.4$.

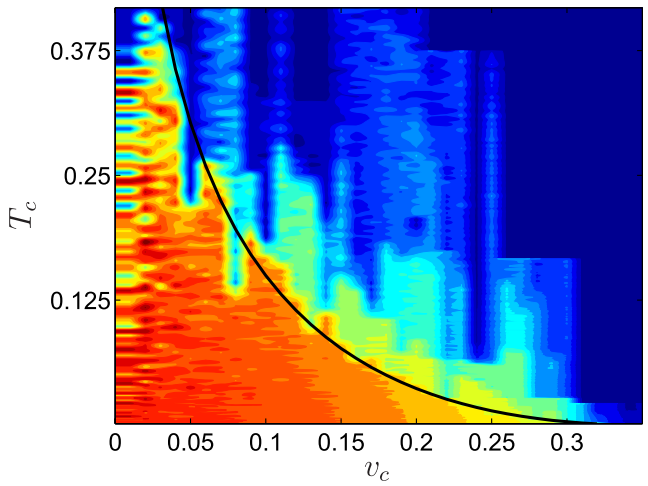

FIG. 5 (color online). Contour plot of the supersolid fraction as a function of temperature and velocity. The solid line corresponds to the critical condition (11), with $v_0 = 0.35$ and the constant of proportionality $\kappa = 0.4$ as fitting parameters.

In conclusion, we have studied the superfluid fraction for the case of dipole-blockaded condensates in the phase of crystalline order, as a double function of the boost speed and thermal fluctuations. It is observed that the data are consistent with a picture of a thermal activation process of superfluid vortices through a nucleation barrier. This result is in contradiction with the interpretation of the experimental data of [13] where the self-similar v and T dependence of the superfluid fraction was understood to be proof of a coupling between elasticity and the NCRI. We also tried to find a self-similar relation, but there was less clear evidence of a correlation between the critical velocity and temperature than that provided by Eq. (11). The present view is, in fact, compatible with the vortex fluid model developed by Anderson [34] and also with recent experiments by Kim *et al.* [35] in three dimensions. In this 3D case (something not possible for dipole-blockaded condensates), the relation (11) must be modified, yielding

$$\frac{\hbar^3}{m^2}\varrho^{ss}\frac{1}{v_c} \propto k_B T_c.$$

Finally, let us emphasize that the characteristic temperatures where the phenomena are observed correspond to 20–30% of the energy scale of the system, which are typically of the order of $\frac{\hbar^2}{m}n_0$ in two-space dimensions. Thus, because of the crystalline structure, the relevant temperatures here are much lower than for liquid superfluid.

We thank Nestor Sepúlveda and Charles Adams for useful discussions throughout the work on this Letter. This work has been supported by Grant No. ANR-08-SYSC-004 (ANR COSTUME) of the Agence National de la Recherche, France. S. R., on leave of absence from Institute Nonlinéaire de Nice (CNRS, France), also acknowledges FONDECYT Grant No. 1100289.

[1] O. Penrose and L. Onsager, Phys. Rev. **104**, 576 (1956).
[2] D. J. Bishop, M. A. Paalanen, and J. D. Reppy, Phys. Rev. B **24**, 2844 (1981).
[3] E. Kim and M. H. W. Chan, Nature (London) **427**, 225 (2004).
[4] E. Kim and M. H. W. Chan, Science **305**, 1941 (2004).
[5] E. Kim and M. H. W. Chan, Phys. Rev. Lett. **97**, 115302 (2006).
[6] Y. Aoki, J. C. Graves, and H. Kojima, Phys. Rev. Lett. **99**, 015301 (2007).
[7] A. Penzev, Y. Yasuta, and M. Kubota, J. Low Temp. Phys. **148**, 677 (2007).
[8] M. Kondo, S. Takada, Y. Shibayama, and K. Shirahama, J. Low Temp. Phys. **148**, 695 (2007).
[9] B. Hunt, E. Pratt, V. Gadagkar, M. Yamashita, A. V.Balatsky, and J. C. Davis, Science **324**, 632 (2009).
[10] A. S. Rittner and J. D. Reppy, Phys. Rev. Lett. **97**, 165301 (2006).
[11] A. S. Rittner and J. D. Reppy, Phys. Rev. Lett. **98**, 175302 (2007).
[12] J. Day and J. Beamish, Nature (London) **450**, 853 (2007).
[13] E. J. Pratt, B. Hunt, V. Gadagkar, M. Yamashita, M. J. Graf, A. V. Balatsky, and J. C. Davis, Science **332**, 821 (2011).
[14] J. R. Beamish, A. D. Fefferman, A. Haziot, X. Rojas, and S. Balibar, Phys. Rev. B **85**, 180501 (2012).
[15] R. Heidemann, U. Raitzsch, V. Bendkowsky, B. Butscher, R. Löw, and T. Pfau, Phys. Rev. Lett. **100**, 033601 (2008).
[16] F. Cinti, P. Jain, M. Boninsegni, A. Micheli, P. Zoller, and G. Pupillo, Phys. Rev. Lett. **105**, 135301 (2010).
[17] See Supplemental Material at http://link.aps.org/supplemental/10.1103/PhysRevLett.109.045301 for derivation of the mean-field dipolar interaction energy.
[18] L. Santos, G. V. Shlyapnikov, and M. Lewenstein, Phys. Rev. Lett. **90**, 250403 (2003).
[19] N. Henkel, R. Nath, and T. Pohl, Phys. Rev. Lett. **104**, 195302 (2010).
[20] G. Pupillo, A. Micheli, M. Boninsegni, I. Lesanovsky, and P. Zoller, Phys. Rev. Lett. **104**, 223002 (2010).
[21] Actually the numerical prefactor of Λ depends on the shape of the potential and an adequate definition is $\Lambda = \frac{n_0 m a^2}{\hbar^2} \int V(|\boldsymbol{x}|) d\boldsymbol{x}$.
[22] N. N. Bogoliubov, J. Phys. USSR **11**, 23 (1947).
[23] C. Josserand, Y. Pomeau, and S. Rica, Phys. Rev. Lett. **98**, 195301 (2007).
[24] C. Josserand, Y. Pomeau, and S. Rica Eur, Eur. Phys. J. Special Topics **146**, 47 (2007).
[25] N. Sepúlveda, C. Josserand, and S. Rica, Eur. Phys. J. B **78**, 439 (2010).
[26] N. Sepúlveda, C. Josserand, and S. Rica, Phys. Rev. B **77**, 054513 (2008).
[27] A. Aftalion, X. Blanc, and R. L. Jerrard, Phys. Rev. Lett. **99**, 135301 (2007).
[28] B. I. Halperin, P. C. Hohenberg, and S. Ma, Phys. Rev. Lett. **29**, 1548 (1972); Phys. Rev. B **10**, 139 (1974);B. I. Halperin, P. C. Hohenberg, and E. Siggia, Phys. Rev. B **13**, 1299 (1976).
[29] P. B. Blakie, A. S. Bradley, M. J. Davis, R. J.Ballagh, and C. W. Gardiner, Adv. Phys. **57**, 363 (2008).
[30] N. Sepúlveda, Phys. Rev. A **83**, 043603 (2011).
[31] G. Krstulovic and M. Brachet, Phys. Rev. E **83**, 066311 (2011).
[32] J. S. Langer and M. E. Fisher, Phys. Rev. Lett. **19**, 560 (1967).
[33] L. Pismen, *Vortices in Nonlinear Fields: From Liquid Crystals to Superfluids, From Non-Equilibrium Patterns to Cosmic Strings* (Clarendon, Oxford, 1999).
[34] P. W. Anderson, Nature Phys. **3**, 160 (2007).
[35] H. Choi, D. Takahashi, K. Kono, and E. Kim, Science **330**, 1512 (2010).